



Search for Gravitational Waves Associated with γ -ray Bursts Detected by the Interplanetary Network

J. Aasi,¹ B. P. Abbott,¹ R. Abbott,¹ T. Abbott,² M. R. Abernathy,¹ F. Acernese,^{3,4} K. Ackley,⁵ C. Adams,⁶ T. Adams,⁷ P. Addesso,⁸ R. X. Adhikari,¹ C. Affeldt,⁹ M. Agathos,¹⁰ N. Aggarwal,¹¹ O. D. Aguiar,¹² P. Ajith,¹³ A. Alemic,¹⁴ B. Allen,^{9,15,16} A. Allocca,^{17,18} D. Amariutei,⁵ M. Andersen,¹⁹ R. A. Anderson,¹ S. B. Anderson,¹ W. G. Anderson,¹⁵ K. Arai,¹ M. C. Araya,¹ C. Arceneaux,²⁰ J. S. Areeda,²¹ S. Ast,¹⁶ S. M. Aston,⁶ P. Astone,²² P. Aufmuth,¹⁶ H. Augustus,²³ C. Aubert,⁹ B. E. Aylott,²³ S. Babak,²⁴ P. T. Baker,²⁵ G. Ballardin,²⁶ S. W. Ballmer,¹⁴ J. C. Barayoga,¹ M. Barbet,⁵ B. C. Barish,¹ D. Barker,²⁷ F. Barone,^{3,4} B. Barr,²⁸ L. Barsotti,¹¹ M. Barsuglia,²⁹ M. A. Barton,²⁷ I. Bartos,³⁰ R. Bassiri,¹⁹ A. Basti,^{31,18} J. C. Batch,²⁷ J. Bauchrowitz,⁹ Th. S. Bauer,¹⁰ C. Baune,⁹ V. Bavigada,²⁶ B. Behnke,²⁴ M. Bejger,³² M. G. Beker,¹⁰ C. Belczynski,³³ A. S. Bell,²⁸ C. Bell,²⁸ G. Bergmann,⁹ D. Bersanetti,^{34,35} A. Bertolini,¹⁰ J. Betzwieser,⁶ I. A. Bilenko,³⁶ G. Billingsley,¹ J. Birch,⁶ S. Biscans,¹¹ M. Bitossi,¹⁸ C. Biwer,¹⁴ M. A. Bizouard,³⁷ E. Black,¹ J. K. Blackburn,¹ L. Blackburn,³⁸ D. Blair,³⁹ S. Bloemen,^{10,40} O. Bock,⁹ T. P. Bodiya,¹¹ M. Boer,⁴¹ G. Bogaert,⁴¹ C. Bogan,⁹ C. Bond,²³ F. Bondu,⁴² L. Bonelli,^{31,18} R. Bonnand,⁴³ R. Bork,¹ M. Born,⁹ V. Boschi,¹⁸ Sukanta Bose,^{44,45} L. Bosi,⁴⁶ C. Bradaschia,¹⁸ P. R. Brady,^{15,47} V. B. Braginsky,³⁶ M. Branchesi,^{48,49} J. E. Brau,⁵⁰ T. Briant,⁵¹ D. O. Bridges,⁶ A. Brillet,⁴¹ M. Brinkmann,⁹ V. Brisson,³⁷ A. F. Brooks,¹ D. A. Brown,¹⁴ D. D. Brown,²³ F. Brückner,²³ S. Buchman,¹⁹ A. Buikema,¹¹ T. Bulik,³³ H. J. Bulten,^{52,10} A. Buonanno,⁵³ R. Burman,³⁹ D. Buskulic,⁴³ C. Buy,²⁹ L. Cadonati,^{54,7} G. Cagnoli,⁵⁵ J. Calderón Bustillo,⁵⁶ E. Calloni,^{57,4} J. B. Camp,³⁸ P. Campsie,²⁸ K. C. Cannon,⁵⁸ B. Canuel,²⁶ J. Cao,⁵⁹ C. D. Capano,⁵³ F. Carbognani,²⁶ L. Carbone,²³ S. Caride,⁶⁰ G. Castaldi,⁸ S. Caudill,¹⁵ M. Cavaglia,²⁰ F. Cavalier,³⁷ R. Cavalieri,²⁶ C. Celerier,¹⁹ G. Cella,¹⁸ C. Cepeda,¹ E. Cesarini,⁶¹ R. Chakraborty,¹ T. Chalermongsak,¹ S. J. Chamberlin,¹⁵ S. Chao,⁶² P. Charlton,⁶³ E. Chassande-Mottin,²⁹ X. Chen,³⁹ Y. Chen,⁶⁴ A. Chincarini,³⁵ A. Chiummo,²⁶ H. S. Cho,⁶⁵ M. Cho,⁵³ J. H. Chow,⁶⁶ N. Christensen,⁶⁷ Q. Chu,³⁹ S. S. Y. Chua,⁶⁶ S. Chung,³⁹ G. Ciani,⁵ F. Clara,²⁷ D. E. Clark,¹⁹ J. A. Clark,⁵⁴ J. H. Clayton,¹⁵ F. Cleva,⁴¹ E. Coccia,^{68,69} P.-F. Cohadon,⁵¹ A. Colla,^{70,22} C. Collette,⁷¹ M. Colombini,⁴⁶ L. Cominsky,⁷² M. Constanancio, Jr.,¹² A. Conte,^{70,22} D. Cook,²⁷ T. R. Corbitt,² N. Cornish,²⁵ A. Corsi,⁷³ C. A. Costa,¹² M. W. Coughlin,⁷⁴ J.-P. Coulon,⁴¹ S. Countryman,³⁰ P. Couvares,¹⁴ D. M. Coward,³⁹ M. J. Cowart,⁶ D. C. Coyne,¹ R. Coyne,⁷³ K. Craig,²⁸ J. D. E. Creighton,¹⁵ R. P. Croce,⁸ S. G. Crowder,⁷⁵ A. Cumming,²⁸ L. Cunningham,²⁸ E. Cuoco,²⁶ C. Cutler,⁶⁴ K. Dahl,⁹ T. Dal Canton,⁹ M. Damjanic,⁹ S. L. Danilishin,³⁹ S. D'Antonio,⁶¹ K. Danzmann,^{16,9} V. Dattilo,²⁶ H. Daveloza,⁷⁶ M. Davier,³⁷ G. S. Davies,²⁸ E. J. Daw,⁷⁷ R. Day,²⁶ T. Dayanga,⁴⁴ D. DeBra,¹⁹ G. Debreczeni,⁷⁸ J. Degallaix,⁵⁵ S. Deléglise,⁵¹ W. Del Pozzo,^{10,23} T. Denker,⁹ T. Dent,⁹ H. Dereli,⁴¹ V. Dergachev,¹ R. De Rosa,^{57,4} R. T. DeRosa,² R. DeSalvo,⁸ S. Dhurandhar,⁴⁵ M. Díaz,⁷⁶ J. Dickson,⁶⁶ L. Di Fiore,⁴ A. Di Lieto,^{31,18} I. Di Palma,⁹ A. Di Virgilio,¹⁸ V. Dolique,⁵⁵ E. Dominguez,⁷⁹ F. Donovan,¹¹ K. L. Dooley,⁹ S. Doravari,⁶ R. Douglas,²⁸ T. P. Downes,¹⁵ M. Drago,^{80,81} R. W. P. Drever,¹ J. C. Driggers,¹ Z. Du,⁵⁹ M. Ducrot,⁴³ S. Dwyer,²⁷ T. Eberle,⁹ T. Edo,⁷⁷ M. Edwards,⁷ A. Effler,² H.-B. Eggenstein,⁹ P. Ehrens,¹ J. Eichholz,⁵ S. S. Eikenberry,⁵ G. Endrőczy,⁷⁸ R. Essick,¹¹ T. Etzel,¹ M. Evans,¹¹ T. Evans,⁶ M. Factourovich,³⁰ V. Fafone,^{68,61} S. Fairhurst,⁷ X. Fan,²⁸ Q. Fang,³⁹ S. Farinon,³⁵ B. Farr,⁸² W. M. Farr,²³ M. Favata,⁸³ D. Fazi,⁸² H. Fehrmann,⁹ M. M. Fejer,¹⁹ D. Feldbaum,^{5,6} F. Feroz,⁷⁴ I. Ferrante,^{31,18} E. C. Ferreira,¹² F. Ferrini,²⁶ F. Fidecaro,^{31,18} L. S. Finn,⁸⁴ I. Fiori,²⁶ R. P. Fisher,¹⁴ R. Flaminio,⁵⁵ J.-D. Fournier,⁴¹ S. Franco,³⁷ S. Frasca,^{70,22} F. Frasconi,¹⁸ M. Frede,⁹ Z. Frei,⁸⁵ A. Freise,²³ R. Frey,⁵⁰ T. T. Fricke,⁹ P. Fritschel,¹¹ V. V. Frolov,⁶ P. Fulda,⁵ M. Fyffe,⁶ J. R. Gair,⁷⁴ L. Gammaitoni,^{86,46} S. Gaonkar,⁴⁵ F. Garufi,^{57,4} N. Gehrels,³⁸ G. Gemme,³⁵ B. Gendre,⁴¹ E. Genin,²⁶ A. Gennai,¹⁸ S. Ghosh,^{10,40} J. A. Giaime,^{6,2} K. D. Giardina,⁶ A. Giazotto,¹⁸ J. Gleason,⁵ E. Goetz,⁹ R. Goetz,⁵ L. Gondan,⁸⁵ G. González,² N. Gordon,²⁸ M. L. Gorodetsky,³⁶ S. Gossan,⁶⁴ S. Goßler,⁹ R. Gouaty,⁴³ C. Gräf,²⁸ P. B. Graff,³⁸ M. Granata,⁵⁵ A. Grant,²⁸ S. Gras,¹¹ C. Gray,²⁷ R. J. S. Greenhalgh,⁸⁷ A. M. Gretarsson,⁸⁸ P. Groot,⁴⁰ H. Grote,⁹ K. Grover,²³ S. Grunewald,²⁴ G. M. Guidi,^{48,49} C. J. Guido,⁶ K. Gushwa,¹ E. K. Gustafson,¹ R. Gustafson,⁶⁰ J. Ha,⁸⁹ E. D. Hall,¹ W. Hamilton,² D. Hammer,¹⁵ G. Hammond,²⁸ M. Hanke,⁹ J. Hanks,²⁷ C. Hanna,^{90,84} M. D. Hannam,⁷ J. Hanson,⁶ J. Harms,¹ G. M. Harry,⁹¹ I. W. Harry,¹⁴ E. D. Harstad,⁵⁰ M. Hart,²⁸ M. T. Hartman,⁵ C.-J. Haster,²³ K. Haughian,²⁸ A. Heidmann,⁵¹ M. Heintze,^{5,6} H. Heitmann,⁴¹ P. Hello,³⁷ G. Hemming,²⁶ M. Hendry,²⁸ I. S. Heng,²⁸ A. W. Heptonstall,¹ M. Heurs,⁹ M. Hewitson,⁹ S. Hild,²⁸ D. Hoak,⁵⁴ K. A. Hodge,¹ D. Hofman,⁵⁵ K. Holt,⁶ P. Hopkins,⁷ T. Horrom,⁹² D. Hoske,⁹³ D. J. Hosken,⁹³ J. Hough,²⁸ E. J. Howell,³⁹ Y. Hu,²⁸ E. Huerta,¹⁴ B. Hughey,⁸⁸ S. Husa,⁵⁶ S. H. Huttner,²⁸ M. Huynh,¹⁵ T. Huynh-Dinh,⁶ A. Idrisy,⁸⁴ D. R. Ingram,²⁷ R. Inta,⁸⁴ G. Islas,²¹ T. Isogai,¹¹ A. Ivanov,¹ B. R. Iyer,⁹⁴ K. Izumi,²⁷ M. Jacobson,¹ H. Jang,⁹⁵ P. Jaranowski,⁹⁶ Y. Ji,⁵⁹ F. Jiménez-Forteza,⁵⁶ W. W. Johnson,² D. I. Jones,⁹⁷ R. Jones,²⁸ R. J. G. Jonker,¹⁰ L. Ju,³⁹ Haris K.,⁹⁸ P. Kalmus,¹ V. Kalogera,⁸² S. Kandhasamy,²⁰ G. Kang,⁹⁵ J. B. Kanner,¹ J. Karlen,⁵⁴

M. Kasprzack,^{37,26} E. Katsavounidis,¹¹ W. Katzman,⁶ H. Kaufer,¹⁶ S. Kaufer,¹⁶ T. Kaur,³⁹ K. Kawabe,²⁷ F. Kawazoe,⁹ F. Kéfélian,⁴¹ G. M. Keiser,¹⁹ D. Keitel,⁹ D. B. Kelley,¹⁴ W. Kells,¹ D. G. Keppel,⁹ A. Khalaidovski,⁹ F. Y. Khalili,³⁶ E. A. Khazanov,⁹⁹ C. Kim,^{89,95} K. Kim,¹⁰⁰ N. G. Kim,⁹⁵ N. Kim,¹⁹ S. Kim,⁹⁵ Y.-M. Kim,⁶⁵ E. J. King,⁹³ P. J. King,¹ D. L. Kinzel,⁶ J. S. Kissel,²⁷ S. Klimenko,⁵ J. Kline,¹⁵ S. Koehlenbeck,⁹ K. Kokeyama,² V. Kondrashov,¹ S. Koranda,¹⁵ W. Z. Korth,¹ I. Kowalska,³³ D. B. Kozak,¹ V. Kringel,⁹ B. Krishnan,⁹ A. Królak,^{101,102} G. Kuehn,⁹ A. Kumar,¹⁰³ D. Nanda Kumar,⁵ P. Kumar,¹⁴ R. Kumar,²⁸ L. Kuo,⁶² A. Kutynia,¹⁰¹ P. K. Lam,⁶⁶ M. Landry,²⁷ B. Lantz,¹⁹ S. Larson,⁸² P. D. Lasky,¹⁰⁴ A. Lazzarini,¹ C. Lazzaro,¹⁰⁵ P. Leaci,²⁴ S. Leavey,²⁸ E. O. Lebigot,⁵⁹ C. H. Lee,⁶⁵ H. K. Lee,¹⁰⁰ H. M. Lee,⁸⁹ J. Lee,¹⁰⁰ P. J. Lee,¹¹ M. Leonardi,^{80,81} J. R. Leong,⁹ I. Leonor,⁵⁰ A. Le Roux,⁶ N. Leroy,^{37,*} N. Letendre,⁴³ Y. Levin,¹⁰⁶ B. Levine,²⁷ J. Lewis,¹ T. G. F. Li,¹ K. Libbrecht,¹ A. Libson,¹¹ A. C. Lin,¹⁹ T. B. Littenberg,⁸² N. A. Lockerbie,¹⁰⁷ V. Lockett,²¹ D. Lodhia,²³ K. Loew,⁸⁸ J. Logue,²⁸ A. L. Lombardi,⁵⁴ E. Lopez,¹⁰⁸ M. Lorenzini,^{68,61} V. Lorette,¹⁰⁹ M. Lormand,⁶ G. Losurdo,⁴⁹ J. Lough,¹⁴ M. J. Lubinski,²⁷ H. Lück,^{16,9} A. P. Lundgren,⁹ Y. Ma,³⁹ E. P. Macdonald,⁷ T. MacDonald,¹⁹ B. Machenschalk,⁹ M. MacInnis,¹¹ D. M. Macleod,² F. Magaña-Sandoval,¹⁴ R. Magee,⁴⁴ M. Mageswaran,¹ C. Maglion, ⁷⁹ K. Mailand,¹ E. Majorana,²² I. Maksimovic,¹⁰⁹ V. Malvezzi,^{68,61} N. Man,⁴¹ G. M. Manca,⁹ I. Mandel,²³ V. Mandic,⁷⁵ V. Mangano,^{70,22} N. M. Mangini,⁵⁴ G. Mansell,⁶⁶ M. Mantovani,¹⁸ F. Marchesoni,^{110,46} F. Marion,⁴³ S. Márka,³⁰ Z. Márka,³⁰ A. Markosyan,¹⁹ E. Maros,¹ J. Marque,²⁶ F. Martelli,^{48,49} I. W. Martin,²⁸ R. M. Martin,⁵ L. Martinelli,⁴¹ D. Martynov,¹ J. N. Marx,¹ K. Mason,¹¹ A. Masserot,⁴³ T. J. Massinger,¹⁴ F. Matichard,¹¹ L. Matone,³⁰ N. Mavalvala,¹¹ G. May,² N. Mazumder,⁹⁸ G. Mazzolo,⁹ R. McCarthy,²⁷ D. E. McClelland,⁶⁶ S. C. McGuire,¹¹¹ G. McIntyre,¹ J. McIver,⁵⁴ K. McLin,⁷² D. Meacher,⁴¹ G. D. Meadors,⁶⁰ M. Mehmet,⁹ J. Meidam,¹⁰ M. Meinders,¹⁶ A. Melatos,¹⁰⁴ G. Mendell,²⁷ R. A. Mercer,¹⁵ S. Meshkov,¹ C. Messenger,²⁸ M. S. Meyer,⁶ P. M. Meyers,⁷⁵ F. Mezzani,^{22,70} H. Miao,⁶⁴ C. Michel,⁵⁵ E. E. Mikhailov,⁹² L. Milano,^{57,4} J. Miller,¹¹ Y. Minenkov,⁶¹ C. M. F. Mingarelli,²³ C. Mishra,⁹⁸ S. Mitra,⁴⁵ V. P. Mitrofanov,³⁶ G. Mitselmakher,⁵ R. Mittleman,¹¹ B. Moe,¹⁵ A. Moggi,¹⁸ M. Mohan,²⁶ S. R. P. Mohapatra,¹⁴ D. Moraru,²⁷ G. Moreno,²⁷ N. Morgado,⁵⁵ S. R. Morriss,⁷⁶ K. Mossavi,⁹ B. Mours,⁴³ C. M. Mow-Lowry,⁹ C. L. Mueller,⁵ G. Mueller,⁵ S. Mukherjee,⁷⁶ A. Mullavey,² J. Munch,⁹³ D. Murphy,³⁰ P. G. Murray,²⁸ A. Mytidis,⁵ M. F. Nagy,⁷⁸ I. Nardecchia,^{68,61} L. Naticchioni,^{70,22} R. K. Nayak,¹¹² V. Necula,⁵ G. Nelemans,^{10,40} I. Neri,^{86,46} M. Neri,^{34,35} G. Newton,²⁸ T. Nguyen,⁶⁶ A. B. Nielsen,⁹ S. Nissanke,⁶⁴ A. H. Nitz,¹⁴ F. Nocera,²⁶ D. Nolting,⁶ M. E. N. Normandin,⁷⁶ L. K. Nuttall,¹⁵ E. Ochsner,¹⁵ J. O'Dell,⁸⁷ E. Oelker,¹¹ J. J. Oh,¹¹³ S. H. Oh,¹¹³ F. Ohme,⁷ S. Omar,¹⁹ P. Oppermann,⁹ R. Oram,⁶ B. O'Reilly,⁶ W. Ortega,⁷⁹ R. O'Shaughnessy,¹⁵ C. Osthelder,¹ D. J. Ottaway,⁹³ R. S. Ottens,⁵ H. Overmier,⁶ B. J. Owen,⁸⁴ C. Padilla,²¹ A. Pai,⁹⁸ O. Palashov,⁹⁹ C. Palomba,²² H. Pan,⁶² Y. Pan,⁵³ C. Pankow,¹⁵ F. Paoletti,^{26,18} M. A. Papa,^{15,24} H. Paris,¹⁹ A. Pasqualetti,²⁶ R. Passaquieti,^{31,18} D. Passuello,¹⁸ M. Pedraza,¹ A. Pele,²⁷ S. Penn,¹¹⁴ A. Perreca,¹⁴ M. Phelps,¹ M. Pichot,⁴¹ M. Pickenpack,⁹ F. Piergiovanni,^{48,49} V. Pierro,⁸ L. Pinard,⁵⁵ I. M. Pinto,⁸ M. Pitkin,²⁸ J. Poeld,⁹ R. Poggiani,^{31,18} A. Poteomkin,⁹⁹ J. Powell,²⁸ J. Prasad,⁴⁵ V. Predoi,⁷ S. Premachandra,¹⁰⁶ T. Prestegard,⁷⁵ L. R. Price,¹ M. Prijatelj,²⁶ S. Privitera,¹ G. A. Prodi,^{80,81} L. Prokhorov,³⁶ O. Puncken,⁷⁶ M. Punturo,⁴⁶ P. Puppo,²² M. Pürner,⁷ J. Qin,³⁹ V. Quetschke,⁷⁶ E. Quintero,¹ R. Quitzow-James,⁵⁰ F. J. Raab,²⁷ D. S. Rabeling,^{52,10} I. Rácz,⁷⁸ H. Radkins,²⁷ P. Raffai,⁸⁵ S. Raja,¹¹⁵ G. Rajalakshmi,¹¹⁶ M. Rakhmanov,⁷⁶ C. Ramet,⁶ K. Ramirez,⁷⁶ P. Rapagnani,^{70,22} V. Raymond,¹ M. Razzano,^{31,18} V. Re,^{68,61} S. Recchia,^{68,69} C. M. Reed,²⁷ T. Regimbau,⁴¹ S. Reid,¹¹⁷ D. H. Reitze,^{1,5} O. Reula,⁷⁹ E. Rhoades,⁸⁸ F. Ricci,^{70,22} R. Riesen,⁶ K. Riles,⁶⁰ N. A. Robertson,^{1,28} F. Robinet,³⁷ A. Rocchi,⁶¹ S. B. Roddy,⁶ L. Rolland,⁴³ J. G. Rollins,¹ R. Romano,^{3,4} G. Romanov,⁹² J. H. Romie,⁶ D. Rosińska,^{118,32} S. Rowan,²⁸ A. Rüdiger,⁹ P. Ruggi,²⁶ K. Ryan,²⁷ F. Salemi,⁹ L. Sammut,¹⁰⁴ V. Sandberg,²⁷ J. R. Sanders,⁶⁰ S. Sankar,¹¹ V. Sannibale,¹ I. Santiago-Prieto,²⁸ E. Saracco,⁵⁵ B. Sassolas,⁵⁵ B. S. Sathyaprakash,⁷ P. R. Saulson,¹⁴ R. Savage,²⁷ J. Scheuer,⁸² R. Schilling,⁹ M. Schilman,⁷⁹ P. Schmidt,⁷ R. Schnabel,^{9,16} R. M. S. Schofield,⁵⁰ E. Schreiber,⁹ D. Schuette,⁹ B. F. Schutz,^{7,24} J. Scott,²⁸ S. M. Scott,⁶⁶ D. Sellers,⁶ A. S. Sengupta,¹¹⁹ D. Sentenac,²⁶ V. Sequino,^{68,61} A. Sergeev,⁹⁹ D. A. Shaddock,⁶⁶ S. Shah,^{10,40} M. S. Shahriar,⁸² M. Shaltev,⁹ Z. Shao,¹ B. Shapiro,¹⁹ P. Shawhan,⁵³ D. H. Shoemaker,¹¹ T. L. Sidery,²³ K. Siellez,⁴¹ X. Siemens,¹⁵ D. Sigg,²⁷ D. Simakov,⁹ A. Singer,¹ L. Singer,¹ R. Singh,² A. M. Sintes,⁵⁶ B. J. J. Slagmolen,⁶⁶ J. Slutsky,³⁸ J. R. Smith,²¹ M. R. Smith,¹ R. J. E. Smith,¹ N. D. Smith-Lefebvre,¹ E. J. Son,¹¹³ B. Sorazu,²⁸ T. Souradeep,⁴⁵ A. Staley,³⁰ J. Stebbins,¹⁹ M. Steinke,⁹ J. Steinlechner,^{9,28} S. Steinlechner,^{9,28} B. C. Stephens,¹⁵ S. Steplewski,⁴⁴ S. Stevenson,²³ R. Stone,⁷⁶ D. Stops,²³ K. A. Strain,²⁸ N. Straniero,⁵⁵ S. Strigin,³⁶ R. Sturani,¹²⁰ A. L. Stuver,⁶ T. Z. Summerscales,¹²¹ S. Susmithan,³⁹ P. J. Sutton,⁷ B. Swinkels,²⁶ M. Tacca,²⁹ D. Talukder,⁵⁰ D. B. Tanner,⁵ J. Tao,² S. P. Tarabrin,⁹ R. Taylor,¹ G. Tellez,⁷⁶ M. P. Thirugnanasambandam,¹ M. Thomas,⁶ P. Thomas,²⁷ K. A. Thorne,⁶ K. S. Thorne,⁶⁴ E. Thrane,¹ V. Tiwari,⁵ K. V. Tokmakov,¹⁰⁷ C. Tomlinson,⁷⁷ M. Tonelli,^{31,18} C. V. Torres,⁷⁶ C. I. Torrie,^{1,28} F. Travasso,^{86,46} G. Traylor,⁶ M. Tse,³⁰ D. Tshilumba,⁷¹ H. Tuennermann,⁹ D. Ugolini,¹²² C. S. Unnikrishnan,¹¹⁶ A. L. Urban,¹⁵ S. A. Usman,¹⁴ H. Vahlbruch,¹⁶ G. Vajente,^{31,18} G. Valdes,⁷⁶ M. Vallisneri,⁶⁴ M. van Beuzekom,¹⁰

J. F. J. van den Brand,^{52,10} C. Van Den Broeck,¹⁰ M. V. van der Sluys,^{10,40} J. van Heijningen,¹⁰ A. A. van Veggel,²⁸ S. Vass,¹ M. Vasúth,⁷⁸ R. Vaulin,¹¹ A. Vecchio,²³ G. Vedovato,¹⁰⁵ J. Veitch,¹⁰ P. J. Veitch,⁹³ K. Venkateswara,¹²³ D. Verkindt,⁴³ F. Vetrano,^{48,49} A. Viceré,^{48,49} R. Vincent-Finley,¹¹¹ J.-Y. Vinet,⁴¹ S. Vitale,¹¹ T. Vo,²⁷ H. Vocca,^{86,46} C. Vorvick,²⁷ W. D. Voudsen,²³ S. P. Vyachanin,³⁶ A. R. Wade,⁶⁶ L. Wade,¹⁵ M. Wade,¹⁵ M. Walker,² L. Wallace,¹ S. Walsh,¹⁵ M. Wang,²³ X. Wang,⁵⁹ R. L. Ward,⁶⁶ M. Was,⁹ B. Weaver,²⁷ L.-W. Wei,⁴¹ M. Weinert,⁹ A. J. Weinstein,¹ R. Weiss,¹¹ T. Welborn,⁶ L. Wen,³⁹ P. Wessels,⁹ M. West,¹⁴ T. Westphal,⁹ K. Wette,⁹ J. T. Whelan,¹²⁴ D. J. White,⁷⁷ B. F. Whiting,⁵ K. Wiesner,⁹ C. Wilkinson,²⁷ K. Williams,¹¹¹ L. Williams,⁵ R. Williams,¹ T. D. Williams,¹²⁵ A. R. Williamson,⁷ J. L. Willis,¹²⁶ B. Willke,^{16,9} M. Wimmer,⁹ W. Winkler,⁹ C. C. Wipf,¹¹ A. G. Wiseman,¹⁵ H. Wittel,⁹ G. Woan,²⁸ N. Wolovick,⁷⁹ J. Worden,²⁷ Y. Wu,⁵ J. Yablon,⁸² I. Yakushin,⁶ W. Yam,¹¹ H. Yamamoto,¹ C. C. Yancey,⁵³ H. Yang,⁶⁴ S. Yoshida,¹²⁵ M. Yvert,⁴³ A. Zadrožny,¹⁰¹ M. Zanolin,⁸⁸ J.-P. Zendri,¹⁰⁵ Fan Zhang,^{11,59} L. Zhang,¹ C. Zhao,³⁹ H. Zhu,⁸⁴ X. J. Zhu,³⁹ M. E. Zucker,¹¹ S. Zuraw,⁵⁴ J. Zweizig,¹ R. L. Apteekar,¹²⁷ J. L. Atteia,^{128,129} T. Cline,³⁸ V. Connaughton,¹³⁰ D. D. Frederiks,¹²⁷ S. V. Golenetskii,¹²⁷ K. Hurley,¹³¹ H. A. Krimm,^{132,133} M. Marisaldi,¹³⁴ V. D. Pal'shin,^{127,135} D. Palmer,¹³⁶ D. S. Svinkin,¹²⁷ Y. Terada,¹³⁷ and A. von Kienlin¹³⁸

(LIGO Scientific Collaboration, Virgo Collaboration, and IPN Collaboration)

¹LIGO, California Institute of Technology, Pasadena, California 91125, USA

²Louisiana State University, Baton Rouge, Louisiana 70803, USA

³Università di Salerno, Fisciano, I-84084 Salerno, Italy

⁴INFN, Sezione di Napoli, Complesso Universitario di Monte S. Angelo, I-80126 Napoli, Italy

⁵University of Florida, Gainesville, Florida 32611, USA

⁶LIGO Livingston Observatory, Livingston, Louisiana 70754, USA

⁷Cardiff University, Cardiff CF24 3AA, United Kingdom

⁸University of Sannio at Benevento, I-82100 Benevento, Italy and INFN, Sezione di Napoli, I-80100 Napoli, Italy

⁹Albert-Einstein-Institut, Max-Planck-Institut für Gravitationsphysik, D-30167 Hannover, Germany

¹⁰Nikhef, Science Park, 1098 XG Amsterdam, The Netherlands

¹¹LIGO, Massachusetts Institute of Technology, Cambridge, Massachusetts 02139, USA

¹²Instituto Nacional de Pesquisas Espaciais, 12227-010 - São José dos Campos, São Paulo, Brazil

¹³International Centre for Theoretical Sciences, Tata Institute of Fundamental Research, Bangalore 560012, India.

¹⁴Syracuse University, Syracuse, New York 13244, USA

¹⁵University of Wisconsin–Milwaukee, Milwaukee, Wisconsin 53201, USA

¹⁶Leibniz Universität Hannover, D-30167 Hannover, Germany

¹⁷Università di Siena, I-53100 Siena, Italy

¹⁸INFN, Sezione di Pisa, I-56127 Pisa, Italy

¹⁹Stanford University, Stanford, California 94305, USA

²⁰The University of Mississippi, University, Mississippi 38677, USA

²¹California State University Fullerton, Fullerton, California 92831, USA

²²INFN, Sezione di Roma, I-00185 Roma, Italy

²³University of Birmingham, Birmingham B15 2TT, United Kingdom

²⁴Albert-Einstein-Institut, Max-Planck-Institut für Gravitationsphysik, D-14476 Golm, Germany

²⁵Montana State University, Bozeman, Montana 59717, USA

²⁶European Gravitational Observatory (EGO), I-56021 Cascina, Pisa, Italy

²⁷LIGO Hanford Observatory, Richland, Washington 99352, USA

²⁸SUPA, University of Glasgow, Glasgow G12 8QQ, United Kingdom

²⁹APC, AstroParticule et Cosmologie, Université Paris Diderot,

CNRS/IN2P3, CEA/Irfu, Observatoire de Paris, Sorbonne Paris Cité, 10,

rue Alice Domon et Léonie Duquet, F-75205 Paris Cedex 13, France

³⁰Columbia University, New York, New York 10027, USA

³¹Università di Pisa, I-56127 Pisa, Italy

³²CAMK-PAN, 00-716 Warsaw, Poland

³³Astronomical Observatory Warsaw University, 00-478 Warsaw, Poland

³⁴Università degli Studi di Genova, I-16146 Genova, Italy

³⁵INFN, Sezione di Genova, I-16146 Genova, Italy

³⁶Faculty of Physics, Lomonosov Moscow State University, Moscow 119991, Russia

³⁷LAL, Université Paris-Sud, IN2P3/CNRS, F-91898 Orsay, France

³⁸NASA/Goddard Space Flight Center, Greenbelt, Maryland 20771, USA

³⁹University of Western Australia, Crawley, Western Australia 6009, Australia

⁴⁰Department of Astrophysics/IMAPP, Radboud University Nijmegen, P.O. Box 9010, 6500 GL Nijmegen, The Netherlands

- ⁴¹*Université Nice-Sophia-Antipolis, CNRS, Observatoire de la Côte d'Azur, F-06304 Nice, France*
- ⁴²*Institut de Physique de Rennes, CNRS, Université de Rennes 1, F-35042 Rennes, France*
- ⁴³*Laboratoire d'Annecy-le-Vieux de Physique des Particules (LAPP), Université de Savoie, CNRS/IN2P3, F-74941 Annecy-le-Vieux, France*
- ⁴⁴*Washington State University, Pullman, Washington 99164, USA*
- ⁴⁵*Inter-University Centre for Astronomy and Astrophysics, Pune - 411007, India*
- ⁴⁶*INFN, Sezione di Perugia, I-06123 Perugia, Italy*
- ⁴⁷*Yukawa Institute for Theoretical Physics, Kyoto University, Kyoto 606-8502, Japan*
- ⁴⁸*Università degli Studi di Urbino 'Carlo Bo', I-61029 Urbino, Italy*
- ⁴⁹*INFN, Sezione di Firenze, I-50019 Sesto Fiorentino, Firenze, Italy*
- ⁵⁰*University of Oregon, Eugene, Oregon 97403, USA*
- ⁵¹*Laboratoire Kastler Brossel, ENS, CNRS, UPMC, Université Pierre et Marie Curie, F-75005 Paris, France*
- ⁵²*VU University Amsterdam, 1081 HV Amsterdam, The Netherlands*
- ⁵³*University of Maryland, College Park, Maryland 20742, USA*
- ⁵⁴*University of Massachusetts Amherst, Amherst, Massachusetts 01003, USA*
- ⁵⁵*Laboratoire des Matériaux Avancés (LMA), IN2P3/CNRS, Université de Lyon, F-69622 Villeurbanne, Lyon, France*
- ⁵⁶*Universitat de les Illes Balears, E-07122 Palma de Mallorca, Spain*
- ⁵⁷*Università di Napoli 'Federico II', Complesso Universitario di Monte S. Angelo, I-80126 Napoli, Italy*
- ⁵⁸*Canadian Institute for Theoretical Astrophysics, University of Toronto, Toronto, Ontario, M5S 3H8, Canada*
- ⁵⁹*Tsinghua University, Beijing 100084, China*
- ⁶⁰*University of Michigan, Ann Arbor, Michigan 48109, USA*
- ⁶¹*INFN, Sezione di Roma Tor Vergata, I-00133 Roma, Italy*
- ⁶²*National Tsing Hua University, Hsinchu 300, Taiwan*
- ⁶³*Charles Sturt University, Wagga Wagga, New South Wales 2678, Australia*
- ⁶⁴*Caltech-CaRT, Pasadena, California 91125, USA*
- ⁶⁵*Pusan National University, Busan 609-735, Korea*
- ⁶⁶*Australian National University, Canberra, ACT 0200, Australia*
- ⁶⁷*Carleton College, Northfield, Minnesota 55057, USA*
- ⁶⁸*Università di Roma Tor Vergata, I-00133 Roma, Italy*
- ⁶⁹*INFN, Gran Sasso Science Institute, I-67100 L'Aquila, Italy*
- ⁷⁰*Università di Roma 'La Sapienza', I-00185 Roma, Italy*
- ⁷¹*University of Brussels, Brussels 1050, Belgium*
- ⁷²*Sonoma State University, Rohnert Park, California 94928, USA*
- ⁷³*The George Washington University, Washington, DC 20052, USA*
- ⁷⁴*University of Cambridge, Cambridge CB2 1TN, United Kingdom*
- ⁷⁵*University of Minnesota, Minneapolis, Minnesota 55455, USA*
- ⁷⁶*The University of Texas at Brownsville, Brownsville, Texas 78520, USA*
- ⁷⁷*The University of Sheffield, Sheffield S10 2TN, United Kingdom*
- ⁷⁸*Wigner RCP, RMKI, H-1121 Budapest, Konkoly Thege Miklós út 29-33, Hungary*
- ⁷⁹*Argentinian Gravitational Wave Group, Cordoba Cordoba 5000, Argentina*
- ⁸⁰*Università di Trento, I-38050 Povo, Trento, Italy*
- ⁸¹*INFN, Gruppo Collegato di Trento, I-38050 Povo, Trento, Italy*
- ⁸²*Northwestern University, Evanston, Illinois 60208, USA*
- ⁸³*Montclair State University, Montclair, New Jersey 07043, USA*
- ⁸⁴*The Pennsylvania State University, University Park, Pennsylvania 16802, USA*
- ⁸⁵*MTA Eötvös University, 'Lendület' A. R. G., Budapest 1117, Hungary*
- ⁸⁶*Università di Perugia, I-06123 Perugia, Italy*
- ⁸⁷*Rutherford Appleton Laboratory, HSIC, Chilton, Didcot, Oxon OX11 0QX, United Kingdom*
- ⁸⁸*Embry-Riddle Aeronautical University, Prescott, Arizona 86301, USA*
- ⁸⁹*Seoul National University, Seoul 151-742, Korea*
- ⁹⁰*Perimeter Institute for Theoretical Physics, Waterloo, Ontario N2 L 2Y5, Canada*
- ⁹¹*American University, Washington, DC 20016, USA*
- ⁹²*College of William and Mary, Williamsburg, Virginia 23187, USA*
- ⁹³*University of Adelaide, Adelaide, South Australia 5005, Australia*
- ⁹⁴*Raman Research Institute, Bangalore, Karnataka 560080, India*
- ⁹⁵*Korea Institute of Science and Technology Information, Daejeon 305-806, Korea*
- ⁹⁶*Białystok University, 15-424 Białystok, Poland*
- ⁹⁷*University of Southampton, Southampton SO17 1BJ, United Kingdom*
- ⁹⁸*IISER-TVM, CET Campus, Trivandrum, Kerala 695016, India*

- ⁹⁹*Institute of Applied Physics, Nizhny Novgorod 603950, Russia*
¹⁰⁰*Hanyang University, Seoul 133-791, Korea*
¹⁰¹*NCBJ, 05-400 Świerk-Otwock, Poland*
¹⁰²*IM-PAN, 00-956 Warsaw, Poland*
¹⁰³*Institute for Plasma Research, Bhat, Gandhinagar 382428, India*
¹⁰⁴*The University of Melbourne, Parkville, VIC 3010, Australia*
¹⁰⁵*INFN, Sezione di Padova, I-35131 Padova, Italy*
¹⁰⁶*Monash University, Victoria 3800, Australia*
¹⁰⁷*SUPA, University of Strathclyde, Glasgow G1 1XQ, United Kingdom*
¹⁰⁸*Louisiana Tech University, Ruston, Louisiana 71272, USA*
¹⁰⁹*ESPCI, CNRS, F-75005 Paris, France*
¹¹⁰*Università di Camerino, Dipartimento di Fisica, I-62032 Camerino, Italy*
¹¹¹*Southern University and A&M College, Baton Rouge, Louisiana 70813, USA*
¹¹²*IISER-Kolkata, Mohanpur, West Bengal 741252, India*
¹¹³*National Institute for Mathematical Sciences, Daejeon 305-390, Korea*
¹¹⁴*Hobart and William Smith Colleges, Geneva, New York 14456, USA*
¹¹⁵*RRCAT, Indore, Madhya Pradesh 452013, India*
¹¹⁶*Tata Institute for Fundamental Research, Mumbai 400005, India*
¹¹⁷*SUPA, University of the West of Scotland, Paisley PA1 2BE, United Kingdom*
¹¹⁸*Institute of Astronomy, 65-265 Zielona Góra, Poland*
¹¹⁹*Indian Institute of Technology, Gandhinagar, Ahmedabad, Gujarat 382424, India*
¹²⁰*Instituto de Física Teórica, Universidade Estadual Paulista/ICTP South American Institute for Fundamental Research, São Paulo, São Paulo 01140-070, Brazil*
¹²¹*Andrews University, Berrien Springs, Michigan 49104, USA*
¹²²*Trinity University, San Antonio, Texas 78212, USA*
¹²³*University of Washington, Seattle, Washington 98195, USA*
¹²⁴*Rochester Institute of Technology, Rochester, New York 14623, USA*
¹²⁵*Southeastern Louisiana University, Hammond, Louisiana 70402, USA*
¹²⁶*Abilene Christian University, Abilene, Texas 79699, USA*
¹²⁷*Ioffe Physical-Technical Institute, Saint Petersburg, 194021, Russian Federation*
¹²⁸*Université de Toulouse, UPS-OMP, IRAP, Toulouse, France*
¹²⁹*CNRS, IRAP, 14, Avenue Edouard Belin, F-31400 Toulouse, France*
¹³⁰*CSPAR, University of Alabama in Huntsville, Huntsville, Alabama 35899, USA*
¹³¹*University of California-Berkeley, Space Sciences Lab, 7 Gauss Way, Berkeley, California 94720, USA*
¹³²*Center for Research and Exploration in Space Science and Technology (CRESSST) and NASA Goddard Space Flight Center, Greenbelt, Maryland 20771, USA*
¹³³*Universities Space Research Association, 7178 Columbia Gateway Drive Columbia, Maryland 21046, USA*
¹³⁴*INAF-IASF Bologna, Via Piero Gobetti 101, 40129 Bologna, Italy*
¹³⁵*Saint Petersburg State Polytechnical University, 195251, Saint Petersburg, Russia*
¹³⁶*Los Alamos National Laboratory, Los Alamos, New Mexico 87545, USA*
¹³⁷*Graduate School of Science and Engineering, Saitama University, Saitama City, Japan*
¹³⁸*Max-Planck-Institut für extraterrestrische Physik, Giessenbachstrasse 1, 85748 Garching, Germany*

(Received 7 April 2014; published 30 June 2014)

We present the results of a search for gravitational waves associated with 223 γ -ray bursts (GRBs) detected by the InterPlanetary Network (IPN) in 2005–2010 during LIGO’s fifth and sixth science runs and Virgo’s first, second, and third science runs. The IPN satellites provide accurate times of the bursts and sky localizations that vary significantly from degree scale to hundreds of square degrees. We search for both a well-modeled binary coalescence signal, the favored progenitor model for short GRBs, and for generic, unmodeled gravitational wave bursts. Both searches use the event time and sky localization to improve the gravitational wave search sensitivity as compared to corresponding all-time, all-sky searches. We find no evidence of a gravitational wave signal associated with any of the IPN GRBs in the sample, nor do we find evidence for a population of weak gravitational wave signals associated with the GRBs. For all IPN-detected GRBs, for which a sufficient duration of quality gravitational wave data are available, we place lower bounds on the distance to the source in accordance with an optimistic assumption of gravitational wave emission energy of $10^{-2}M_{\odot}c^2$ at 150 Hz, and find a median of 13 Mpc. For the 27 short-hard GRBs we place 90% confidence exclusion distances to two source models: a binary neutron star coalescence, with a median distance of 12 Mpc, or the coalescence of a neutron star and black hole, with a median distance of 22 Mpc. Finally, we combine this search with

previously published results to provide a population statement for GRB searches in first-generation LIGO and Virgo gravitational wave detectors and a resulting examination of prospects for the advanced gravitational wave detectors.

DOI: [10.1103/PhysRevLett.113.011102](https://doi.org/10.1103/PhysRevLett.113.011102)

PACS numbers: 04.80.Nn, 07.05.Kf, 95.85.Sz, 98.70.Rz

γ -ray bursts (GRBs) are amongst the most energetic electromagnetic astrophysical phenomena. They fall into two commonly accepted groups depending on their duration and spectral hardness [1,2] and are referred to as “short” or “long.” Short GRBs (duration less than 2 s, hard spectra) are believed to be produced by the mergers of either double neutron star or neutron-star–black-hole binaries [1], and the recent observation of a kilonova associated with GRB130603B [3,4] lends support to this hypothesis. Such compact binary coalescences generate strong gravitational waves (GWs) in the sensitive frequency band of Earth-based gravitational wave detectors [5,6]. The detection of gravitational waves associated with a short GRB would provide direct evidence that the progenitor is indeed a coalescing compact binary as well as distinguish between a double neutron star (NSNS) and neutron-star–black-hole (NSBH) progenitor. Long GRBs (duration greater than 2 s, soft spectra) models are mostly related to the collapse of rapidly rotating massive stars. The extreme conditions encountered in such objects may make the system susceptible to a variety of rotational instabilities that may emit up to $10^{-2}M_{\odot}c^2$ through GW radiation [7,8].

Between 2005 and 2010, the first generation of large-scale interferometric gravitational wave detectors—LIGO, Virgo, and GEO—were operating at, or close to, their design sensitivities. During these runs, the detectors had a sensitivity out to tens of Mpc for binary mergers [9–12] and other transients emitting $10^{-2}M_{\odot}c^2$ in gravitational waves [13–15].

Although it is expected that most GRB progenitors observed by γ -ray detectors will be at distances too large for the resulting gravitational wave signals to be detectable by initial LIGO and Virgo [16,17], it is possible that in the GRB data set under study that one might be within the range of the detectors. For example, the smallest observed redshift to date of an optical GRB afterglow is $z = 0.0085$ (≈ 36 Mpc) for GRB 980425 [18–20]; this would be within the LIGO-Virgo detectable range for some progenitor models. Although GRB 980425 is a long duration soft spectrum GRB, observations seem to suggest that, on average, short-duration GRBs tend to have smaller redshifts than long GRBs [21,22]. We therefore search for evidence of a gravitational wave signal associated with any observed short or long GRB for which there is a sufficient duration of high-quality data in at least two detectors. By making use of the known time and sky location of the observed GRB, it is possible to significantly reduce the parameters of the search and consequently improve the sensitivity over an all-sky, all-time search of the data. Several searches for gravitational

waves associated with γ -ray bursts have been performed in the past using data from both LIGO and Virgo detectors [23–27]. Indeed, the data from LIGO’s fifth and sixth science runs (S5 and S6) and Virgo’s first through third science runs (VSR1-3) were analyzed to search for gravitational wave signals associated with both short and long GRBs observed with the *Swift* BAT and *Fermi* GBM and LAT detectors [28–30]. No evidence for a gravitational wave signal was found in these searches.

The InterPlanetary Network (IPN) [31] is a group of satellites orbiting the Earth, Mars, and Mercury and operating, among other equipment on board, γ -ray detectors. The IPN, in its current configuration, acts as a quasi-all-sky and full-time γ -ray burst detector. Thus, the IPN provides an additional population of GRBs which may not be observed solely by *Swift* or *Fermi* and tends to detect brighter (therefore, on average, closer) bursts, which are relevant for gravitational wave searches. The IPN provides accurate GRB times as well as sky locations determined by triangulation between the satellites in the network. Depending upon the satellites involved, the localization can vary from less than one square degree to over one thousand. Two short duration GRBs, GRB 051103 [32,33] and GRB 070201 [34], were localized by the IPN with error boxes overlapping the M81 galaxy at 3.6 Mpc and the Andromeda galaxy (M31) at 770 kpc, respectively. The gravitational wave data around the times of these GRBs were analyzed in [35] and [36], respectively. The non-detection of associated gravitational waves ruled out the progenitor object being a binary merger in M81 or M31 with over 99% confidence.

In this Letter we present the results of a targeted search for gravitational waves around the burst trigger times of 223 additional γ -ray bursts, including 27 short GRBs, localized by the InterPlanetary Network (IPN) during both LIGO’s fifth and Virgo’s first science runs (S5 and VSR1) and LIGO’s sixth and Virgo’s second and third science runs (S6 and VSR2-3). The search for gravitational wave bursts (GWBs) is performed on all the GRBs, short or long, for which we have good-quality gravitational wave data, regardless of the localization error box size. In addition, a search for a binary merger signal is performed for the 27 short hard GRBs for which there was sufficiently good sky localization to make the search tractable.

We find no evidence for a gravitational wave candidate associated with any of the IPN GRBs in this sample, and statistical analyses of the GRB sample rule out the presence of a collective signature of weak gravitational waves associated with the GRB population. We place lower

bounds on the distance to the progenitor for each GRB, and constrain the fraction of the observed GRB population at low redshifts. Additionally, we combine the results presented here with those from previous analyses to provide a comprehensive limit from all of the GRB searches. Using this, we extrapolate to the future advanced detector network and show that the observation of a gravitational wave signal associated with a GRB is possible, but by no means guaranteed and the continued all sky coverage provided by the IPN will increase these chances.

GRB sample.—The Interplanetary Network (IPN) is a group of spacecraft equipped with γ -ray detectors used to localize γ -ray bursts (GRBs) and soft γ repeaters (SGRs, or magnetars). The IPN has contributed burst data to LIGO since the initial engineering runs in 2001. At the time of this combined search, nine spacecraft contribute their data: *Wind*, *Mars Odyssey*, *MESSENGER*, *INTEGRAL*, *RHESSI*, *Swift*, *Suzaku*, *AGILE* and *Fermi*.

The astronomical locations of GRBs are determined by comparing the relative arrival times of the signal at the spacecraft. The precision is inversely proportional to the spacecraft separations, among other things, so that the localization accuracy of a network with baselines of thousands of light-seconds can be equal to or superior to that of any other technique. A description of the error box construction process can be found in [37] and, specific to our search, in [38]. The light curves, energy spectra, and localizations of all the bursts in our sample were examined to eliminate the possibility of contamination by magnetar bursts or solar flares. None of these events have been followed up by x-ray or optical telescopes, so no information on afterglows or possible host galaxies and associated redshifts is available. The full list of GRBs and their parameters can be found in the Supplemental Material [39] associated with the Letter.

The classification of GRBs into long or short typically uses the T_{90} duration for a given detector. This is defined as the time interval over which 90% of the total background-subtracted photon counts are accumulated. However, this time depends on the energy range to which the detector is sensitive and may therefore vary across the satellites observing the bursts. Since the IPN bursts are observed by a set of different detectors with different sensitivities, to quote a single T_{90} for them could be misleading. Even when a single detector measures this time, it is possible to get different numbers for the same burst depending on the arrival angle, which affects the sensitivity as a function of energy. In this analysis, where possible, we have used the classification provided by [40], based on observations with Konus-Wind. We note that the set of short bursts observed by Konus is split into type I (likely merger scenario), possibly with extended emission, and type II (collapsar). For the modeled search, we only analyzed the type I bursts. For bursts not observed by Konus, the T_{90} observed by *Suzaku* was used and in cases where this was not available,

a by-eye estimate of duration from another mission with good sensitivity (such as *Swift* or *INTEGRAL*) was used. In these cases, any burst with a T_{90} under two seconds was classified as short. The unmodeled search uses many minutes of data around the given time of the burst, whereas the modeled search uses a small six-second window around “short” bursts to search for the binary coalescence, due to the predicted time difference between merger and GRB emission. It is therefore important that the time of arrival at the Earth be calculated as accurately as possible for these bursts. When the burst is observed by a near-Earth satellite, this is straightforward and approximated to the spacecraft time. However, for some poorly localized GRBs only observed by distant satellites, the uncertainty in the Earth-crossing time can be up to approximately five seconds.

Only the GRBs that occurred when two or more of the LIGO and Virgo detectors were operating in a stable configuration are analyzed. Gravitational-wave data segments that are flagged as being of poor quality are excluded from the analysis. Thus, although the IPN observed over 600 bursts during the period of interest, only 223 could be analyzed, of which 27 are classified as short. This nevertheless constitutes the largest GRB sample used to date in such a study.

Gravitational wave detectors.—In this Letter, we discuss results obtained from analyzing data collected by the initial LIGO and Virgo gravitational wave detectors. There were three LIGO detectors: a 4 km and a 2 km detector, both at Hanford, Washington, (referred to as H1 and H2, respectively) and another 4 km detector in Livingston, Louisiana (L1). The Virgo detector is a 3 km detector located in Cascina, Italy. Details of these detectors can be found in [41] and [42]. From 2005 to 2010, these detectors were operating at or near design sensitivity. The fifth LIGO science run (S5) took place from November 2005 to August 2007 and the sixth science run (S6) ran from June 2009 to October 2010. The second Hanford detector (H2) was not operational during S6. Virgo operated three distinct science runs during this time: VSR1 ran from May to October 2007, VSR2 ran from July 2009 to January 2010, and VSR3 ran from August to October 2010.

The existence of multiple, widely separated detectors around the globe aids our ability to localize signals in blind, all-sky searches. Additionally, noise artifacts in the detectors caused by terrestrial disturbances are likely to be uncorrelated between the detectors, aiding the ability to distinguish true signals from the noise background. The Hanford and Livingston detectors are separated by 3000 km, which corresponds to 10 ms travel time for light or gravitational waves. The Hanford and Virgo observatories are separated by 27 ms and the Livingston and Virgo observatories by 26 ms.

Search methodology.—The methods used to search for binary merger signals and GWBs are largely the same as for the previous analysis described in [30]. The one major

change is the necessity to search the variably shaped, irregularly sized error regions provided by the IPN localizations. We begin by describing how that is done and then provide a brief review of the remainder of the analysis details, referring the reader to [30] for more details.

Covering the error boxes: The analysis of the gravitational wave data depends on the assumed sky direction to the GRB, since the data must be time-shifted according to the expected time-of-arrival at each detector. This is also weighted by the response of each GW detector to the assumed sky direction. Each GRB localization error box corresponds to a 3σ region determined by the intersection of the IPN timing annuli, with a construction process described in detail in [38]. However, most of these IPN error regions are larger than the directional resolution of the GW detector network. Thus, to maximize the likelihood of finding a gravitational wave signal associated with the GRB, we perform a discrete search across the entire IPN error box by populating it with a grid of points and repeating the search at each of these points. The GW detectors have a timing resolution of ~ 0.5 ms, corresponding to a spatial resolution of a few degrees. Therefore, we chose search point separations of approximately 3.6 degrees when only LIGO interferometers' data were used in the search and 1.8 degrees when the more widely separated Virgo detector was also used. The probability distributions of search points over the error boxes were chosen Gaussian for long bursts (to assure that there are proportionally more points for those positions with larger probabilities of containing a signal) and uniform for short bursts (no assumptions made in terms of signal origin within the error box). Short GRBs which could not be localized to better than a few hundred square degrees were not analyzed in the modeled search due to high computational requirements and the negligible increase in sensitivity rendered by a targeted search. We use simulated signals to determine the sensitivity of our searches. We distribute these over the IPN error boxes, with the density of simulations weighted according to the estimated source position probability distribution. This assures that there are proportionally more simulations for those positions with larger probabilities of being the true GRB signal location.

During the S5 run, two LIGO detectors, H1 and H2, were operational at the Hanford site. There are a number of bursts for which the only available gravitational wave data are from these two detectors. Since the detectors are co-located and co-aligned, it is not possible to distinguish different sky locations based on the observed gravitational wave signal. In this case, there is no need to perform an explicit search over the error box and, for the binary search, all such GRBs can be analyzed.

Search for GWs from a compact binary progenitor: For the binary merger progenitor model, it is believed that the delay between the merger and the emission of γ rays will be small [see discussion in [30]]. We therefore search for

binary coalescences with a merger time between 5 s prior to the GRB and 1 s afterwards. This is wide enough to allow for potential precursors, some uncertainties in the emission model and in the arrival time of the electromagnetic signal at the IPN spacecraft, as well as for the differences in sensitivity of the IPN detectors. In addition, we require a minimum of 40 minutes of data available around the time of the GRB. This ensures both that the detectors were operating stably at the time as well as providing a set of comparable data which can be used to estimate the background of noise events.

For the short GRBs, the data streams from the operational detectors are combined coherently and searched by matched-filtering against a bank of binary merger gravitational waveforms, as described in [43]. The gravitational waveform emitted by a binary system depends on the masses and spins of the NS and its companion (either NS or BH), as well as on the distance to the source, its sky position, inclination angle, and the polarization angle of the orbital axis. As described above, we tile the sky region with a fixed set of points to search, and we similarly tile the mass space [44] to provide sensitivity to binaries with component masses greater than $1M_{\odot}$ with an upper limit of $3M_{\odot}$ for any neutron star and a total mass of $25M_{\odot}$. The remaining parameters are handled by maximizing the likelihood analytically over these dimensions. In addition to matched filtering, the analysis utilizes a number of signal consistency tests to reject nonstationary, transient noise “glitches” in the GW detectors' data [43].

Search for gravitational wave bursts: The procedure used to search for generic short-duration ($\lesssim 1$ s) GW bursts follows that used in previous GRB analyses [30,45]. All GRBs are treated identically regardless of their classification. We search for a GW event between 600 s prior to the GRB trigger time and 60 s after or the T_{90} time, whichever is greater. This timescale allows us to take into account almost all of the possible scenarios for a GW emission associated with the GRB; see [30] for more details. Since the GWB search requires more data around the GRB than the binary merger search, there are GRBs for which we can perform the merger search but not the search for unmodeled transients. The data within a ± 1.5 h window around the GRB is used to estimate the background of noise events in the data. The search for a GWB between 60 and 500 Hz is performed by the X-PIPELINE algorithm [46,47]. Candidate events are then ranked based on their energy and a number of signal consistency tests are applied to reduce the effect of nonstationary noise seen in the GW detectors. Events occurring at times of known instrumental problems or environmental disturbances are discarded.

Significance of results: The significance of any candidate gravitational wave event is estimated by using the data surrounding the GRB time. Specifically, we divide the surrounding data into a large number of blocks of identical length to the search region and calculate the false alarm

probability (FAP), or p value of the event by counting the fraction of off-source trials with an event louder than the one observed. Where necessary, we artificially time-shift the data from the detectors by several seconds to generate more off-source trials that can be used to estimate the background.

In addition to a single, significant event, it's possible that the data could contain several weak signals. In order to test whether this is the case, we use a weighted distribution of observed p values and see whether it is consistent with the expected, uniform distribution of noise. We also use a weighted binomial test to more quantitatively assess consistency with the no-signal hypothesis. This test looks for deviations from the null hypothesis in the 5% tail of lowest p values weighted by the prior probability of detection (estimated from the GW search sensitivity). This combination allows us to give more weight to those GRBs for which the gravitational wave network was most sensitive, which are the ones we are most likely to detect. The result of the weighted binomial test is compared with the distribution obtained from simulated results with p values uniformly distributed in $[0, 1]$ to evaluate the population significance. The test is described in greater detail in the appendix of [30] and in [47].

Results.—A search for gravitational waves has been performed for a total of 223 GRBs. Of these, 27 were classified as short GRBs with a likely binary coalescence progenitor. The gravitational wave data at the time of these GRBs has been searched for evidence of the coalescence waveforms. For 221 bursts, including 25 of the 27 short bursts we have performed a search for generic gravitational wave transients in the IPN error box around the time of the GRB. A full list of all GRBs analyzed is available in the supplementary material, where we provide two tables listing the short and long GRBs analyzed in this search.

Modeled coalescing binary search results: For each GRB, we estimate the p values of the gravitational wave candidate, by comparing with the background trials. The distribution of observed p values is shown in Fig. 1. No significant candidates found. The p value is estimated from the background. However, for a number of GRBs, particularly those observed in the colocated Hanford detectors, the search yields no candidate gravitational wave events after background rejection cuts. For such GRBs, when no event is observed, we cannot quote an exact p value but only a range bounded below by the fraction of background trials with an event and above by 1. The result of the weighted binomial population detection test yields a background probability of $\approx 98\%$, strongly favoring the no-signal hypothesis. In conclusion, no noteworthy individual events were found by this search, nor evidence for a collective population of weak gravitational wave signals.

Unmodeled GW burst results: The unmodeled gravitational wave burst pipeline analyzed both short and long GRBs. The distribution of p values for each of the 221 IPN

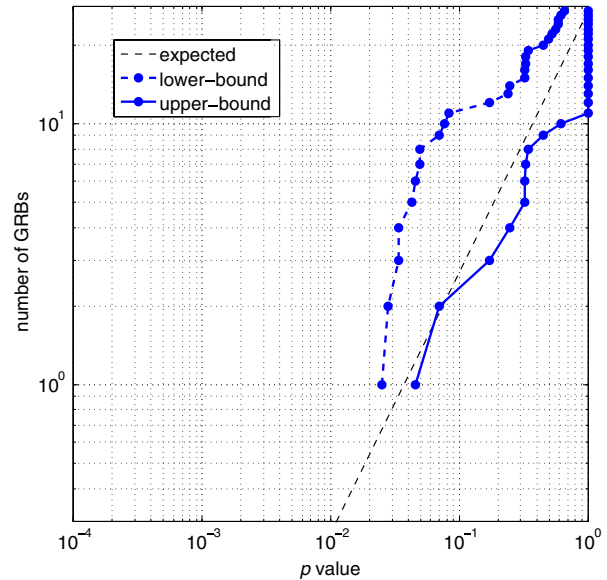


FIG. 1 (color online). Cumulative distribution of p values from the analysis of 27 short-duration IPN GRBs for evidence of a binary merger gravitational wave signal. The expected distribution under the no-signal hypothesis is indicated by the dashed line. For GRBs with no event in the on-source region, we provide upper bounds on the p value equal to 1.

GRBs analyzed is shown in Fig. 2. The binomial test yields a background probability of 68%, consistent with the null hypothesis. The smallest p value, 0.5%, came from GRB060203B, which is statistically consistent with a no-signal hypothesis given the number analyzed.

Astrophysical interpretation.—Given that no significant event was found in our analyses, we place limits on GW

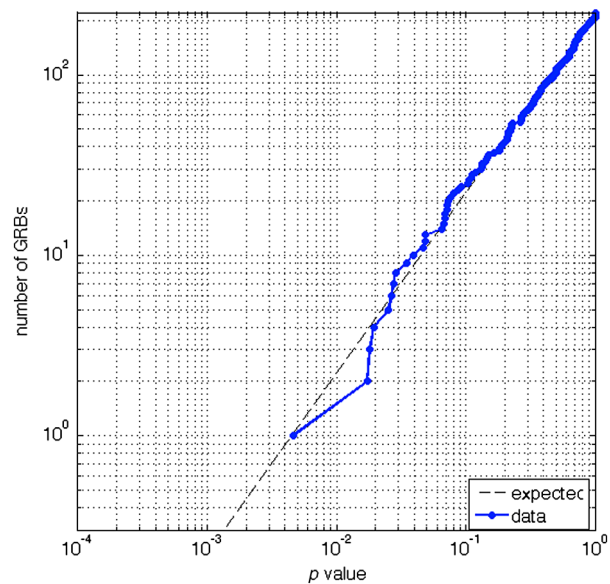


FIG. 2 (color online). Cumulative distribution of p values from the analysis of 221 IPN GRBs for evidence of a gravitational wave transient associated to the burst. The expected distribution under the no-signal hypothesis is indicated by the dashed line.

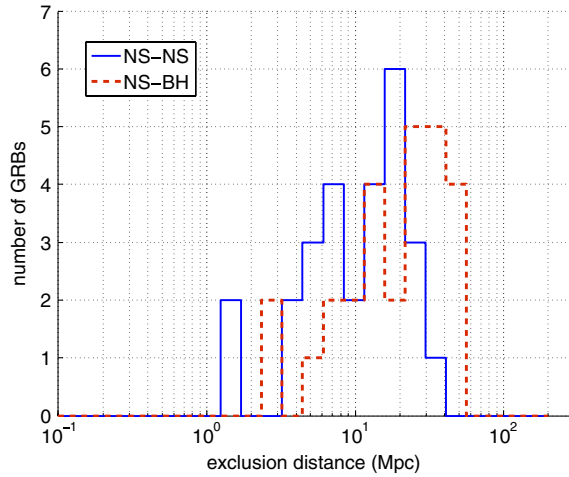


FIG. 3 (color online). Histograms across the sample of short IPN GRBs of the distance exclusions at the 90% confidence level for NS-NS and NS-BH systems.

emission based on both binary merger (for short GRBs) and generic gravitational wave burst (for all GRBs) signal models, and assess the potential of a similar search with second-generation gravitational wave detectors around 2015–2020.

Distance exclusion: For a given signal morphology, the gravitational wave analysis is efficient in recovering signals up to a certain distance limit that depends on the sensitivity of the detectors at the time of the search. We quote a 90% confidence level lower limit on the distance to each GRB progenitor: that is, the distance at which we recover 90% of simulated signals. The quoted exclusion distances are marginalized over systematic errors that are inherent in this analysis: errors introduced by the mismatch of a true GW signal and the waveforms used in the simulations [9] and amplitude errors from the calibration of the detector data [48].

For the short GRBs, we calculate a distance exclusion for both two neutron stars (NSNS) and a neutron star with a black hole (NSBH). In both cases, we assume a jet half-opening angle of 30°, and assume that the GRB is emitted in the direction of the binary’s total angular momentum. The median exclusion distance for NSNS is 12 Mpc and for NSBH is 22 Mpc. A histogram of their values is shown in Fig. 3. The NS masses are chosen from a Gaussian distribution centered at $1.4M_{\odot}$ [49,50] with a width of $0.2M_{\odot}$ for the NSNS case, and a broader spread of $0.4M_{\odot}$ for the NSBH systems, to account for larger uncertainties given the lack of observations for such systems. The BH masses are Gaussian distributed with a mean of $10M_{\odot}$ and a width of $6M_{\odot}$. The BH mass is restricted such that the total mass of the system is less than $25M_{\odot}$. For masses greater than this distribution, the NS would be swallowed without disruption by the BH, no massive torus would form, and no GRB would be produced [51–53]. The dimensionless NS spins are drawn uniformly over

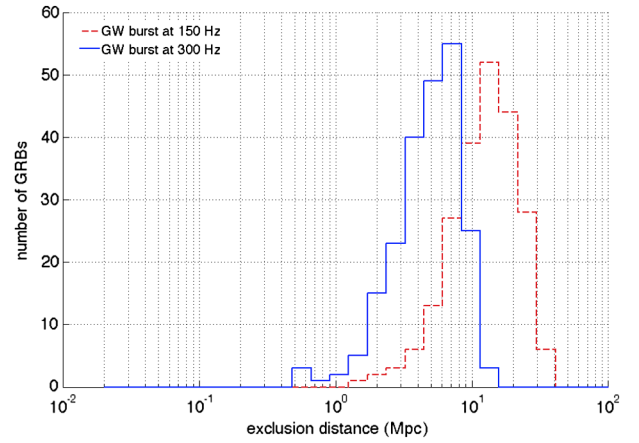


FIG. 4 (color online). Histograms across the sample of IPN GRBs of the distance exclusions at the 90% confidence level for circularly polarized sine-Gaussian GW burst models at 150 and 300 Hz. We assume an optimistic standard siren GW emission of $E_{\text{GW}} = 10^{-2}M_{\odot}c^2$.

[0, 0.4], and the BH spins are drawn uniformly over [0, 0.98) with tilt angle $< 60^{\circ}$.

For the GWB search, no specific waveform model is assumed. Consequently, we use generic signal morphologies to give an idea of the search sensitivity. Specifically, we use circularly polarized sine Gaussians with central emission frequencies of 150 and 300 Hz. We assume a jet opening angle of 5°, which is appropriate for long GRBs. We also assume a total GW emission of $10^{-2}M_{\odot}c^2$; this corresponds to the most optimistic models for gravitational wave emission from long GRBs [30]. The median exclusion distance is 13.0 Mpc at 150 Hz and 4.9 Mpc at 300 Hz, and histograms of the distributions are given in Fig. 4.

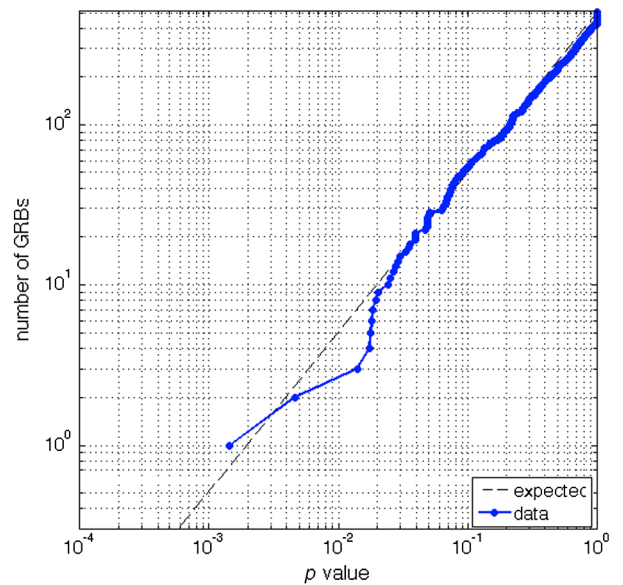


FIG. 5 (color online). Cumulative distribution of p values from the analysis of 508 GRBs. The expected distribution under the no-signal hypothesis is indicated by the dashed line.

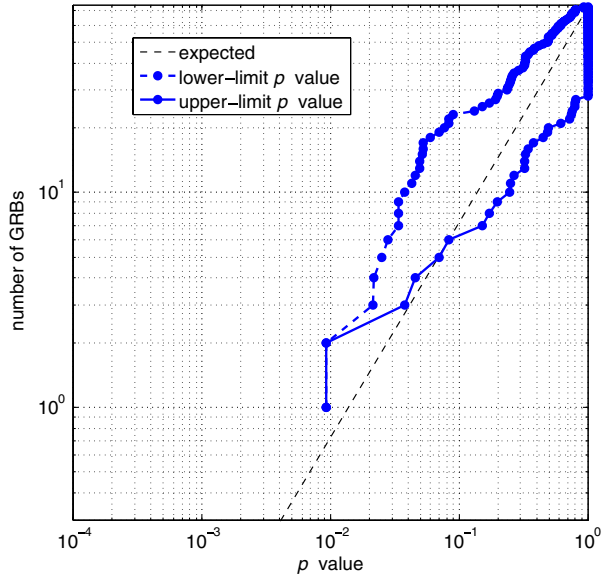


FIG. 6 (color online). Cumulative distribution of p values for all 69 analyzed short GRBs. The expected distribution under the no-signal hypothesis is indicated by the dashed line. For GRBs with no event in the on-source region, we provide upper bounds on the p value of 1.

Population exclusion from all GRBs analyzed: Here we present the combination of all S5-6 and VSR1-3 searches for coincident GRB and GW signals from this Letter, the S5 GRB search [28,29] and the recent S6 and VSR2-3 search [30]. Algorithms which were used for the first S5 paper were adjusted and reviewed to make sure all analyses were comparable. In total, 508 GRBs were analyzed with the burst search and 69 short GRBs were analyzed for a compact binary coalescence GW signal. None of the separate searches showed evidence of a population of weak events. Figures 5 and 6 show the distribution of p values of the full set of GRBs. The weighted binomial test applied to the full population of GRBs confirms that the observed distributions are consistent with the null hypothesis (no signal being observed).

Next, we use the full population of GRBs to place exclusions on GRB populations. To do this, we use a simple population model, where all GRB progenitors have the same GW emission (standard sirens), and perform exclusion on cumulative distance distributions. We parameterize the distance distribution with two components: a fraction F of GRBs distributed with a constant comoving density rate up to a luminosity distance R , and a fraction $1 - F$ at effectively infinite distance. This simple model yields a parameterization of astrophysical GRB distance distribution models that predict a uniform local rate density and a more complex dependence at redshift > 0.1 , as the large-redshift part of the distribution is well beyond the sensitivity of current GW detectors. The exclusion is then performed in the (F, R) plane. For details of this method, see Appendix B of [30].

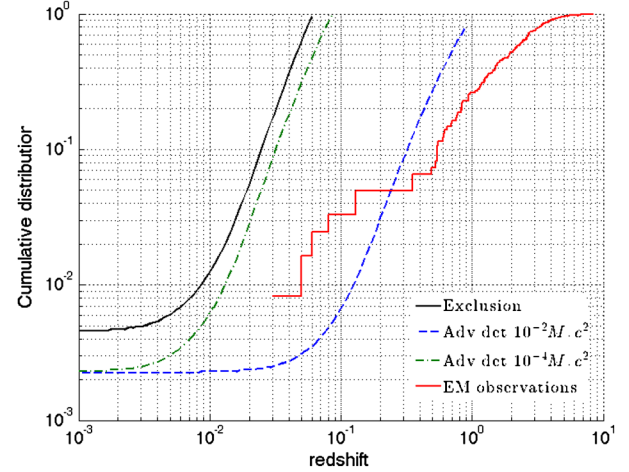


FIG. 7 (color online). Cumulative redshift distribution $F(R)$ exclusion from the analysis of 508 GRBs with the GW burst search. We exclude at 90% confidence level cumulative distance distributions which pass through the region above the black solid curve. We assume a standard siren sine-Gaussian GW burst at 150 Hz with an energy of $E_{\text{GW}} = 10^{-2} M_{\odot} c^2$. We extrapolate this exclusion to Advanced LIGO and Virgo detectors assuming a factor 10 improvement in sensitivity and a factor 2 increase in number of GRB triggers analyzed. The blue dashed curve is the extrapolation assuming the same standard siren energy of $E_{\text{GW}} = 10^{-2} M_{\odot} c^2$ and the green (gray) dashed curve assuming a less optimistic standard siren energy of $E_{\text{GW}} = 10^{-4} M_{\odot} c^2$ [54,55]. For reference, the red staircase curve shows the cumulative distribution of measured redshifts for *Swift* GRBs [56,57].

In Fig. 7 we show the exclusion for GW bursts, using as a reference signal a 150 Hz sine-Gaussian signal, with an energy in gravitational waves of $10^{-2} M_{\odot} c^2$. In addition, we plot the redshift distribution of GRBs as observed by *Swift*. The exclusion at low redshift is dictated by the number of GRBs analyzed and at high redshift by the typical sensitive range of the search. These exclusions assume 100% purity of the GRB sample. In Figure 8, we show the exclusion for the NSNS and NSBH sources. In neither case does the exclusion line come close to the observed population redshift, indicating that it would have been unlikely to observe an event in this analysis. Indeed, an analysis of all IPN bursts shows that their average redshift is 1.7, and that it detects short bursts with good efficiency up to a redshift of about 0.45.

The advanced LIGO and Virgo detectors are nearing completion. They are expected to start taking data in 2015 and reach their design sensitivity towards the end of the decade [58]. We can use the results obtained here to extrapolate and predict what might be expected with the advanced detectors. The S5-6 and VSR1-3 runs comprised a total of around 21 months of two (or more) detector duty cycle. Over that period, the detectors' reach varied by approximately a factor of 4, from a 5 Mpc sensitive distance to NSNS sources for H2 in early S5 to 20 Mpc for H1 and L1 by the end of S6. Similarly, the current scenario [58]

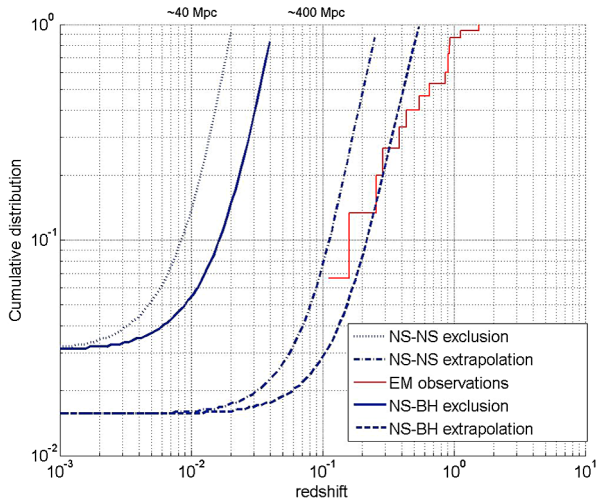


FIG. 8 (color online). Cumulative distance exclusion for 69 analyzed short GRBs for both a NSNS and a NSBH progenitor model. The exclusion distance is given for this test then extrapolated by a factor of two in number and ten in sensitivity for the advanced detector era expectations. For reference, the red staircase curve shows the cumulative distribution of measured redshifts for *Swift* GRBs [56,57].

calls for around 18 months of science runs of ever increasing sensitivity during the commissioning phase, prior to extended running at design sensitivity which will provide a reach roughly ten times what was achieved in S6 and VSR2-3.

To approximate the expected advanced detector results, we scale the exclusion distances obtained here by a factor of ten and also increase by a factor of two the number of observed GRBs to account for the increased run time of a few years. These extrapolated curves are also shown on Figs. 7 and 8. We see that for both generic burst signals and binary mergers, the exclusion curves are now comparable with the observed redshifts. In the optimistic scenario where every GRB emits $10^{-2}M_{\odot}c^2$ of energy in gravitational waves, we will expect to see several such signals, or alternatively be able to exclude this scenario. However, since the $10^{-4}M_{\odot}c^2$ predicted exclusion is to the left of the observed redshifts, we will be unlikely to observe a gravitational wave associated to a GRB if this is the typical amplitude. For binary mergers, the NSNS and NSBH extrapolations bracket the line of observed redshifts, indicating that we might expect to see one (or fewer) NSNS associated with a GRB, but might expect several if NSBH are the progenitors. (These extrapolations are broadly comparable to those obtained using only the S6 and VSR2-3 [30]. They are, however, slightly more pessimistic as they use a more realistic estimate of the evolution of detector sensitivity, as described above.)

Of course, all of the above relies heavily on the continued operation of all sky sensitivity to GRBs, and reasonable localization ability. *Swift* and *Fermi* will continue to run, and SVOM is expected in the advanced

detector timeline, but it's clear that the addition of the all-sky, full-time IPN will aid these searches as well.

Conclusion.—We have performed a search for gravitational waves coincident with 223 γ -ray bursts localized by the InterPlanetary Network between 2005 and 2010. These GRBs were detected by the IPN during LIGO's fifth and sixth science runs and Virgo's first, second, and third science runs. Of these, we analyzed the 27 short GRBs with a focused search that looked for gravitational wave signals from the merger of neutron-star–neutron-star or neutron-star–black-hole binaries, as most likely expected for short GRBs. We also performed an unmodeled burst search over 221 GRBs, both short and long. No gravitational wave was detected in coincidence with a GRB, and lower limits on the distance were set for each GRB for various gravitational wave emission models.

Finally, we have combined these results with those of previous analyses for GRBs during S5-6 and VSR1-3 to provide a comprehensive statement on gravitational wave emission by GRBs from the first-generation LIGO and Virgo detectors. We also extrapolate this exclusion distance for the advanced detector era, where we assume a factor of 2 increase in GRBs and a factor of 10 improvement in sensitivity. This shows that the advanced detector era will begin to exclude certain expected models and possibly make coincident gravitational wave detections with GRBs. These results and prospects for the advanced detector era demonstrate the benefit of searches triggered by γ -ray burst observatories with high sky coverage such as the InterPlanetary Network. The continued operation of these satellites will be crucial in future coincident GRB and gravitational wave searches and increase the likelihood of a detection in the advanced detector era.

The authors gratefully acknowledge the support of the United States National Science Foundation for the construction and operation of the LIGO Laboratory, the Science and Technology Facilities Council of the United Kingdom, the Max Planck Society, and the State of Niedersachsen, Germany, for support of the construction and operation of the GEO600 detector and the Italian Istituto Nazionale di Fisica Nucleare and the French Centre National de la Recherche Scientifique for the construction and operation of the Virgo detector. The authors also gratefully acknowledge the support of the research by these agencies and by the Australian Research Council, the International Science Linkages program of the Commonwealth of Australia, the Council of Scientific and Industrial Research of India, the Istituto Nazionale di Fisica Nucleare of Italy, the Spanish Ministerio de Economía y Competitividad, the Conselleria d'Economia Hisenda i Innovació of the Govern de les Illes Balears, the Foundation for Fundamental Research on Matter supported by the Netherlands Organisation for Scientific Research, the Polish Ministry of Science and Higher Education, the FOCUS Programme of Foundation for Polish Science,

the Royal Society, the Scottish Funding Council, the Scottish Universities Physics Alliance, The National Aeronautics and Space Administration, the Carnegie Trust, the Leverhulme Trust, the David and Lucile Packard Foundation, the Research Corporation, and the Alfred P. Sloan Foundation. K. H. acknowledges IPN support from the following sources: NASA NNX06AI36G, NNX08AB84G, NNX08AZ85G, NNX09AV61G, and NNX10AR12G (*Suzaku*), NASA NNG06GI89G, NNX07AJ65G, NNX08AN23G, NNX09AO97G, NNX10AI23G (*Swift*), NASA NNG06GE69G, NNX07AQ22G, NNX08AC90G, NNX08AX95G, NNX09AR28G (*INTEGRAL*). The Konus-Wind experiment is partially supported by a Russian Space Agency contract and RFBR Grants No. 12-02-00032-a and No. 13-02-12017-ofi_m. This document has been assigned LIGO Laboratory document number LIGO-P1300226-v10.

*Corresponding author.
leroy@lal.in2p3.fr

- [1] E. Nakar, *Phys. Rep.* **442**, 166 (2007).
 [2] Y. P. Qinx, A. C. Gupta, J. H. Fan, C. Y. Su, and R. J. Lu, *Sci. China Phys. Mech. Astron.* **53**, 1375 (2010).
 [3] N. R. Tanvir, A. J. Levan, A. S. Fruchter, J. Hjorth, R. A. Hounsell, K. Wiersema, and R. L. Tunnicliffe, *Nature (London)* **500**, 547 (2013).
 [4] E. Berger, W. Fong, and R. Chornock, *Astrophys. J.* **774**, L23 (2013).
 [5] L. Blanchet, B. R. Iyer, and B. Joguet, *Phys. Rev. D* **65**, 064005 (2002).
 [6] L. Blanchet and T. Damour, *Annales Inst. H. Poincaré Phys. Théor.* **50**, 377 (1989).
 [7] M. Modjaz, *Astron. Nachr.* **332**, 434 (2011).
 [8] J. Hjorth and J. S. Bloom, in *Gamma-Ray Bursts*, edited by C. Kouveliotou, R. A. M. J. Wijers, and S. Woosley, Cambridge Astrophysics Series Vol. 51 (Cambridge University Press, Cambridge, 2012), pp. 169–190.
 [9] B. Abbott *et al.* (LIGO Scientific Collaboration), *Phys. Rev. D* **79**, 122001 (2009).
 [10] B. Abbott *et al.* (LIGO Scientific Collaboration), *Phys. Rev. D* **80**, 047101 (2009).
 [11] J. Abadie *et al.* (LIGO Scientific Collaboration, Virgo Collaboration), *Phys. Rev. D* **82**, 102001 (2010).
 [12] J. Abadie *et al.* (LIGO Collaboration, Virgo Collaboration), *Phys. Rev. D* **85**, 082002 (2012).
 [13] B. Abbott *et al.* (LIGO Scientific Collaboration), *Phys. Rev. D* **80**, 102001 (2009).
 [14] J. Abadie *et al.* (LIGO Collaboration, Virgo Collaboration), *Phys. Rev. D* **81**, 102001 (2010).
 [15] J. Abadie *et al.* (LIGO Scientific Collaboration, Virgo Collaboration), *Phys. Rev. D* **85**, 122007 (2012).
 [16] E. Berger *et al.*, *Astrophys. J.* **634**, 501 (2005).
 [17] B. Metzger and E. Berger, *Astrophys. J.* **746**, 48 (2012).
 [18] S. R. Kulkarni, D. A. Frail, M. H. Wieringa, R. D. Ekers, E. M. Sadler, R. M. Wark, J. L. Higdon, E. S. Phinney, and J. S. Bloom, *Nature (London)* **395**, 663 (1998).
 [19] T. J. Galama *et al.*, *Nature (London)* **395**, 670 (1998).
 [20] K. Iwamoto *et al.*, *Nature (London)* **395**, 672 (1998).
 [21] D. Guetta and T. Piran, *Astron. Astrophys.* **435**, 421 (2005).
 [22] D. B. Fox *et al.*, *Nature (London)* **437**, 845 (2005).
 [23] B. Abbott *et al.*, *Phys. Rev. D* **72**, 042002 (2005).
 [24] B. Abbott *et al.*, *Phys. Rev. D* **77**, 062004 (2008).
 [25] F. Acernese *et al.*, *Classical Quantum Gravity* **24**, S671 (2007).
 [26] F. Acernese *et al.*, *Classical Quantum Gravity* **25**, 225001 (2008).
 [27] J. Aasi *et al.*, *Phys. Rev. D* **88**, 122004 (2013).
 [28] B. Abbott *et al.* (Virgo Collaboration), *Astrophys. J.* **715**, 1438 (2010).
 [29] J. Abadie *et al.* (LIGO Scientific Collaboration, Virgo Collaboration), *Astrophys. J.* **715**, 1453 (2010).
 [30] J. Abadie *et al.*, *Astrophys. J.* **760**, 12 (2012).
 [31] K. Hurley *et al.*, *AIP Conf. Proc.* **662**, 473 (2003).
 [32] D. D. Frederiks, V. D. Palshin, R. L. Aptekar, S. V. Golenetskii, T. L. Cline, and E. P. Mazets, *Astron. Lett.* **33**, 19 (2007).
 [33] K. Hurley *et al.*, *Mon. Not. R. Astron. Soc.* **403**, 342 (2010).
 [34] E. P. Mazets, R. L. Aptekar, T. L. Cline, D. D. Frederiks, J. O. Goldsten, S. V. Golenetskii, K. Hurley, A. von Kienlin, and V. D. Pal'shin, *Astrophys. J.* **680**, 545 (2008).
 [35] J. Abadie *et al.* (The LIGO Scientific Collaboration), *Astrophys. J.* **755**, 2 (2012).
 [36] B. Abbott *et al.* (LIGO Scientific Collaboration), *Astrophys. J.* **681**, 1419 (2008).
 [37] K. Hurley *et al.*, *Astrophys. J.* **537**, 953 (2000).
 [38] V. Predoi (for the LIGO Scientific Collaboration and Virgo Collaboration) and K. Hurley (for the IPN), *J. Phys. Conf. Ser.* **363**, 012034 (2012).
 [39] See Supplemental Material at <http://link.aps.org/supplemental/10.1103/PhysRevLett.113.011102> for the list of analyzed GRBs and their parameters.
 [40] V. Pal'shin, K. Hurley, D. Svinkin, R. Aptekar, S. Golenetskii, *et al.*, *Astrophys. J. Suppl. Ser.* **207**, 38 (2013).
 [41] B. Abbott *et al.*, *Rep. Prog. Phys.* **72**, 076901 (2009).
 [42] T. Accadia *et al.*, *JINST* **7**, P03012 (2012).
 [43] I. W. Harry and S. Fairhurst, *Phys. Rev. D* **83**, 084002 (2011).
 [44] B. J. Owen and B. S. Sathyaprakash, *Phys. Rev. D* **60**, 022002 (1999).
 [45] B. Abbott *et al.*, *Astrophys. J.* **715**, 1438 (2010).
 [46] P. J. Sutton *et al.*, *New J. Phys.* **12**, 053034 (2010).
 [47] M. Waş, Ph.D. thesis, Laboratoire de l'Accélérateur Linéaire, 2011.
 [48] J. Abadie *et al.* (LIGO Scientific Collaboration), *Nucl. Instrum. Methods Phys. Res., Sect. A* **624**, 223 (2010).
 [49] B. Kiziltan, A. Kottas, M. De Yoreo, and S. E. Thorsett, *Astrophys. J.* **778**, 66 (2013).
 [50] F. Ozel, D. Psaltis, R. Narayan, and A. S. Villarreal, *Astrophys. J.* **757**, 55 (2012).
 [51] V. Ferrari, L. Gualtieri, and F. Pannarale, *Phys. Rev. D* **81**, 064026 (2010).
 [52] M. D. Duez, *Classical Quantum Gravity* **27**, 114002 (2010).
 [53] M. Shibata and K. Taniguchi, *Living Rev. Relativity* **14** (2011).

- [54] C. D. Ott, A. Burrows, L. Dessart, and E. Livne, *Phys. Rev. Lett.* **96**, 201102 (2006).
- [55] G. E. Romero, M. M. Reynoso, and H. R. Christiansen, *Astron. Astrophys.* **524**, A4 (2010).
- [56] P. Jakobsson *et al.*, *Astron. Astrophys.* **447**, 897 (2006).
- [57] P. Jakobsson, J. Hjorth, D. Malesani, R. Chapman, J. P. U. Fynbo, N. R. Tanvir, B. Milvang-Jensen, P. M. Vreeswijk, G. Letawe, and R. L. C. Starling, *Astrophys. J.* **752**, 62 (2012).
- [58] J. Aasi *et al.* (LIGO Scientific Collaboration, Virgo Collaboration), [arXiv:1304.0670](https://arxiv.org/abs/1304.0670).